# JOC Featured Article

Discovery and Development of a Small Molecule Library with Lumazine Synthase Inhibitory Activity

Arindam Talukdar,[†] Meghan Breen,[†] Adelbert Bacher,[‡] Boris Illarionov,[§] Markus Fischer,[§] Gunda Georg,[⊥] Qi-Zhuang Ye,[⊥] and Mark Cushman*,[†]

[†]*Department of Medicinal Chemistry and Molecular Pharmacology, School of Pharmacy and Pharmaceutical Sciences, and The Purdue Cancer Center, Purdue University, West Lafayette, Indiana 47907, [‡]Ikosatec GmbH, Königsbergerstr. 74, 85748 Garching, Germany, [§]Institute of Food Chemistry, University of Hamburg, D-20146 Hamburg, Germany, and [⊥]Department of Medicinal Chemistry, University of Kansas, Lawrence, Kansas 66047*

cushman@pharmacy.purdue.edu

Received February 5, 2009

Substrate — HTS Hit Compound — Optimized Inhibitor
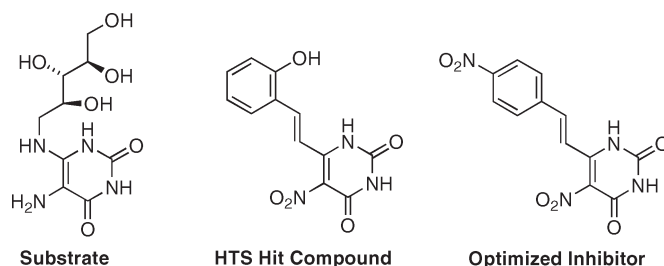
(E)-5-Nitro-6-(2-hydroxystyryl)pyrimidine-2,4(1H,3H)-dione (**9**) was identified as a novel inhibitor of *Schizosaccharomyces pombe* lumazine synthase by high-throughput screening of a 100000 compound library. The K_i of **9** vs *Mycobacterium tuberculosis* lumazine synthase was 95 μM. Compound **9** is a structural analogue of the lumazine synthase substrate 5-amino-6-(D-ribitylamino)-2,4-(1H,3H)pyrimidinedione (**1**). This indicates that the ribitylamino side chain of the substrate is not essential for binding to the enzyme. Optimization of the enzyme inhibitory activity through systematic structure modification of the lead compound **9** led to (E)-5-nitro-6-(4-nitrostyryl)pyrimidine-2,4(1H,3H)-dione (**26**), which has a K_i of 3.7 μM vs *M. tuberculosis* lumazine synthase.

Introduction

Riboflavin (**4**, vitamin B$_2$) plays a crucial role in many biological processes, including photosynthesis and mitochondrial electron transport. While animals obtain riboflavin from dietary sources, numerous microorganisms, including Gram-negative pathogenic bacteria and yeasts, lack an efficient riboflavin uptake system and are therefore absolutely dependent on endogenous riboflavin biosynthesis.[1−4] Riboflavin biosynthesis therefore offers attractive targets for the design and synthesis of new antibiotics, which are urgently needed because pathogens are becoming drug-resistant at an alarming rate.

Lumazine synthase and riboflavin synthase catalyze the last two steps in the biosynthesis of riboflavin (**4**) (Scheme 1). Lumazine synthase catalyzes the condensation of 3,4-dihydroxy-2-butanone 4-phosphate (**2**) with 5-amino-6-ribitylamino-2,4(1H,3H)pyrimidinedione (**1**), yielding 6,7-dimethyl-8-D-ribityllumazine (**3**).[5,6] The final step in the biosynthesis involves a mechanistically unusual dismutation of two molecules of **3**, resulting in the formation of one molecule of riboflavin (**4**) and one molecule of the

(1) Wang, A. *Yichuan Xuebao* **1992**, *19*, 362–368.
(2) Oltmanns, O.; Lingens, F. *Z. Naturforsch.* **1967**, *22 b*, 751–754.
(3) Logvinenko, E. M.; Shavlovsky, G. M. *Mikrobiologiya* **1967**, *41*, 978–979.
(4) Neuberger, G.; Bacher, A. *Biochem. Biophys. Res. Commun.* **1985**, *127*, 175–181.
(5) Neuberger, G.; Bacher, A. *Biochem. Biophys. Res. Commun.* **1986**, *139*, 1111–1116.
(6) Kis, K.; Volk, R.; Bacher, A. *Biochemistry* **1995**, *34*, 2883–2892.

SCHEME 1
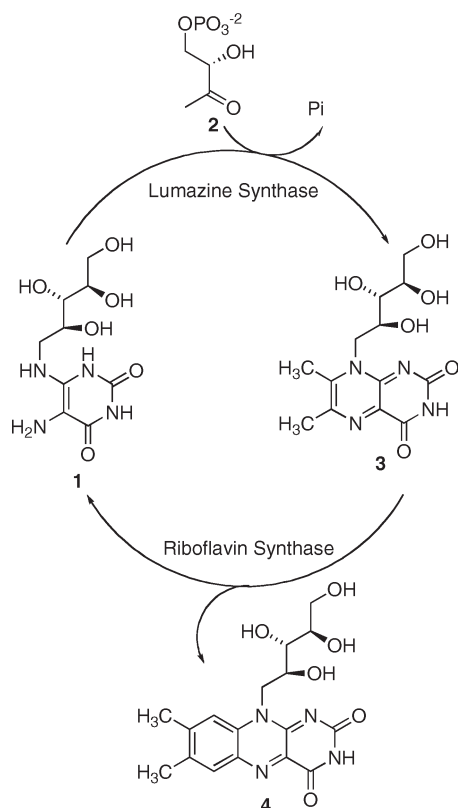
pyrimidinedione derivative **1**, which can then be recycled by lumazine synthase.[7−15]

Although the details of the reaction catalyzed by lumazine synthase have not been completely elucidated, a reasonable pathway can be outlined at the present time as depicted in Scheme 2. Condensation of the primary amino group of the substituted pyrimidinedione **1** with the ketone **2** to give Schiff base **5**, elimination of phosphate to yield the enol **6**, tautomerization of the enol **6** and isomerization of the imine to produce the ketone **7**, ring closure, and dehydration of the covalent hydrate **8** provide the product **3**.[16] It can be assumed that the inorganic phosphate formed after elimination from **5** would remain enzyme bound, at least for some time, but that it would eventually have to be removed to make room for another molecule of the substrate **2**. The present uncertainties revolve around the timing of phosphate elimination and the conformational reorganization of the side chain leading to intermediate **7**.

SCHEME 2
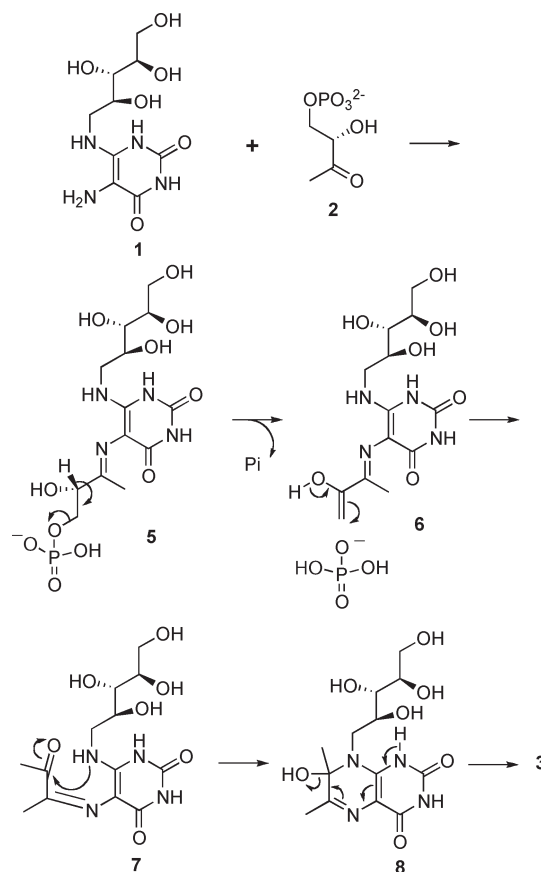
A high-throughput screening (HTS) technique was developed on the basis of competitive binding of lumazine synthase inhibitors and riboflavin to the active site of *Schizosaccharomyces pombe* lumazine synthase.[17,18] The capacity of the *S. pombe* lumazine synthase to bind riboflavin is unique. Free riboflavin is fluorescent with high quantum yield, while enzyme-bound riboflavin is not.[19] Thus, displacement of riboflavin from the binding pocket results in a significant fluorescence increase of the system. The change in fluorescence caused by competitive binding between riboflavin and other ligands for *S. pombe* lumazine synthase was used to identify lumazine synthase inhibitors.[17] All of the known inhibitors tested were positively identified, which confirmed the authenticity of this assay. HTS of a commercial 100000 compound library yielded some interesting results, including the identification of a lead compound **9**.

The thermodynamic HTS assay described above effectively bypasses the problems associated with the instabilities of the lumazine synthase substrates **1** and **2**, and it also simplifies the assay by removing the time element. However, practically speaking, it had two limitations: (1) assay mixtures contained traces of free riboflavin that produced a

(7) Fischer, M.; Haase, I.; Feicht, R.; Schramek, N.; Kohler, P.; Schieberle, P.; Bacher, A. *Biol. Chem.* **2005**, *386*, 417–428.

(8) Gerhardt, S.; Schott, A.-K.; Kairies, N.; Cushman, M.; Illarionov, B.; Eisenreich, W.; Bacher, A.; Huber, R.; Steinbacher, S.; Fischer, M. *Structure* **2002**, *10*, 1371–1381.

(9) Illarionov, B.; Eisenreich, W.; Bacher, A. *Proc. Natl. Acad. Sci. U.S. A.* **2001**, *98*, 7224–7229.

(10) Illarionov, B.; Eisenreich, W.; Schramek, N.; Bacher, A.; Fischer, M. *J. Biol. Chem.* **2005**, *280*, 28541–28546.

(11) Illarionov, B.; Kemter, K.; Eberhardt, S.; Richter, G.; Cushman, M.; Bacher, A. *J. Biol. Chem.* **2001**, *276*, 11524–11530.

(12) Maley, G. F.; Plaut, G. W. E. *J. Biol. Chem.* **1959**, *234*, 641–647.

(13) Plaut, G. W. E. *J. Biol. Chem.* **1963**, *238*, 2225–2243.

(14) Plaut, G. W. E.; Harvey, R. A. *Methods Enzymol.* **1971**, *18B*, 515–538.

(15) Wacker, H.; Harvey, R. A.; Winestock, C. H.; Plaut, G. W. E. *J. Biol. Chem.* **1964**, *239*, 3493–3497.

(16) Volk, R.; Bacher, A. *J. Am. Chem. Soc.* **1988**, *110*, 3651–3653.

(17) Chen, J.; Illarionov, B.; Bacher, A.; Fischer, M.; Haase, I.; Georg, G.; Ye, Q.-z.; Ma, Z.; Cushman, M. *Anal. Biochem.* **2005**, *338*, 124–130.

(18) Kaiser, J.; Illarionov, B.; Rohdich, F.; Eisenreich, W.; Saller, S.; Van den Brulle, J.; Cushman, M.; Bacher, A.; Fischer, M. *Anal. Biochem.* **2007**, *365*, 52–61.

(19) Fischer, M.; Haase, I.; Feicht, R.; Richter, G.; Gerhardt, S.; Changeux, J.-P.; Huber, R.; Bacher, A. *Eur. J. Biochem.* **2002**, *269*, 519–526.
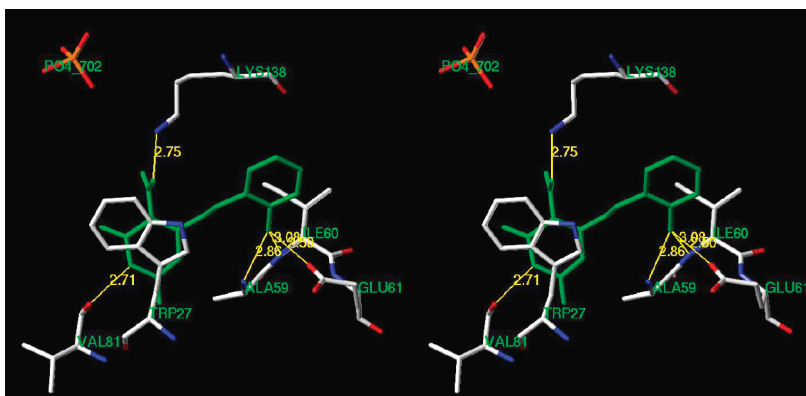
FIGURE 1. Hypothetical model of the complex of the lead compound **9** with *M. tuberculosis* lumazine synthase. The distances shown are in Å. The diagram is programmed for wall-eyed (relaxed) viewing.

fluorescent background, and (2) lumazine synthase inhibitors that bind outside the active site would probably be unable to release free riboflavin. In spite of these problems, the thermodynamic assay remained the method of choice for screening thousands of compounds, and the activities of the hit compounds were confirmed in secondary assays involving classical enzyme kinetics.

Our specific interest in compound **9** is the result of its structural similarity to the substrate **1**. The identification of **9** as a lumazine synthase inhibitor represents an extension of ongoing work on the synthesis of metabolically stable intermediates in the lumazine synthase-catalyzed reaction.[20-23] The HTS hit compound **9** demonstrates that the ribitylamino chain present in the substrate, which was thought to be necessary for binding to the enzyme, can be replaced by a simple hydroxystyryl moiety with retention of lumazine synthase inhibitory activity. The difference in physical properties between compounds **1** and **9** has significant implications for antibiotic drug development. Substrate analogues with ribityl side chains are not suitable as drug candidates because their hydrophilic nature can be expected to prevent them from penetrating bacterial cell walls. Gram-negative bacterial cell walls contain an outer membrane composed of phospholipids and lipopolysaccharides that face toward the external environment. Replacing the hydrophilic ribityl side chain of compound **1** with the styryl moiety renders compound **9** more lipophilic, which should facilitate the entry of the compound into bacteria. Compound **9** displayed K_i values of 210 μM vs *S. pombe* lumazine synthase and 95 μM vs *Mycobacterium tuberculosis* lumazine synthase. Thus, there is ample room for designing more potent lumazine synthase inhibitors based on the structure of the lead compound **9**. Moreover, the lead compound **9** is a substrate analogue of the lumazine synthase-catalyzed reaction, but it is also a product analogue of the riboflavin synthase-catalyzed reaction. Structural analogues of **9** might therefore be expected to inhibit riboflavin synthase as well as lumazine

synthase. Enzyme assays were therefore performed using the riboflavin synthases of *M. tuberculosis* and *E. coli*. In order to help define the spectrum of activity, lumazine synthase inhibition assays were also performed on *M. tuberculosis* lumazine synthase as well as *S. pombe* lumazine synthase.
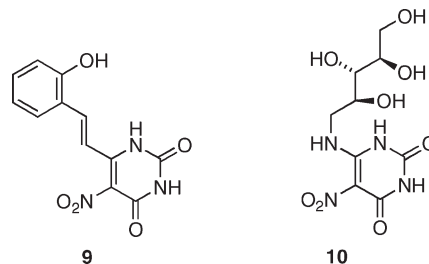
Results and Discussion

The lumazine synthase inhibitory activity of the HTS hit compound **9** might be related to the presence of the phenolic hydroxy on the aromatic ring, which could possibly mimic one of the ribityl hydroxyl groups of the substrate **1**. In addition, it is known that the substrate analogue **10**, which also contains a nitro group, has high affinity for the active site of lumazine synthase and has been crystallized in complex with *Bacillus subtilis* lumazine synthase.[24,25] Molecular modeling was performed in order to investigate the binding mode of the hit compound **9** to the enzyme. The lead compound **9** was docked into the active site of the structure of *M. tuberculosis* lumazine synthase[26,27] using GOLD software (BST, version 3.0, 2005), and energy minimization was then performed with Sybyl 7.1. The resulting structure is displayed in Figure 1. According to this hypothetical model, the binding of the hit compound **9** in the active site of *M. tuberculosis* lumazine synthase is similar to that of substrate and product analogues.[26-28] The structure

(20) Zhang, Y. L.; Illarionov, B.; Morgunova, E.; Jin, G. Y.; Bacher, A.; Fischer, M.; Ladenstein, R.; Cushman, M. *J. Org. Chem.* **2008**, *73*, 2715–2724.

(21) Talukdar, A.; Illarionov, B.; Bacher, A.; Fischer, M.; Cushman, M. *J. Org. Chem.* **2007**, *72*, 7167–7175.

(22) Zhang, Y. L.; Jin, G. Y.; Illarionov, B.; Bacher, A.; Fischer, M.; Cushman, M. *J. Org. Chem.* **2007**, *72*, 7176–7184.

(23) Chen, J.; Sambaiah, T.; Illarionov, B.; Fischer, M.; Bacher, A.; Cushman, M. *J. Org. Chem.* **2004**, *69*, 6996–7003.

(24) Bacher, A.; Ludwig, H. C. *Eur. J. Biochem.* **1982**, *127*, 539–545.

(25) Ritsert, K.; Huber, R.; Turk, D.; Ladenstein, R.; Schmidt-Bäse, K.; Bacher, A. *J. Mol. Biol.* **1995**, *253*, 151–167.

(26) Morgunova, K.; Meining, W.; Illarionov, B.; Haase, I.; Jin, G.; Bacher, A.; Cushman, M.; Fischer, M.; Ladenstein, R. *Biochemistry* **2005**, *44*, 2746–2758.

(27) Morgunova, E.; Illarionov, B.; Sambaiah, T.; Haase, I.; Bacher, A.; Cushman, M.; Fischer, M.; Ladenstein, R. *FEBS J.* **2006**, *273*, 4790–4804.

(28) Gerhardt, S.; Haase, I.; Steinbacher, S.; Kaiser, J. T.; Cushman, M.; Bacher, A.; Huber, R.; Fischer, M. *J. Mol. Biol.* **2002**, *318*, 1317–1329.

SCHEME 3
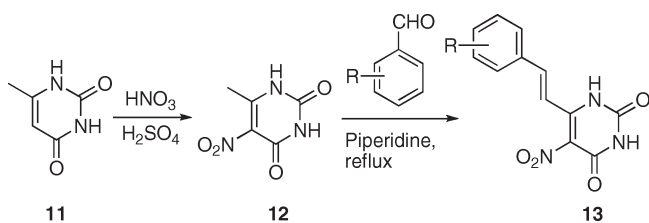
SCHEME 4
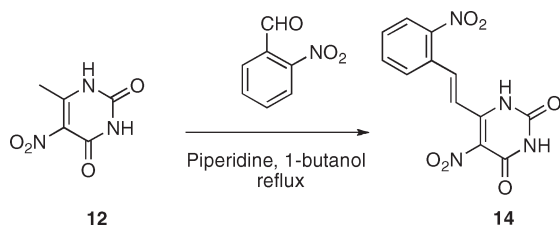
involves hydrogen bonding of the phenolic hydroxyl group of **9** with Ala59, Ile60, and Glu61. In addition, stacking interactions involving Trp27 stabilize the binding. The molecular modeling results indicate that the binding of hit compound **9** in the active site of *M. tuberculosis* lumazine synthase is certainly plausible, and it most likely resembles the known crystal structure of the complex formed between the related substrate analogue **10** and the enzyme.

We have attempted to employ versatile methods that would allow the efficient synthesis of a wide variety of target molecules. Accordingly, an array of aromatic aldehydes were condensed with 6-methyl-5-nitrouracil to afford a focused library of alkenes with pure trans geometry.[29−31] No attempt was made to synthesize cis alkenes because the preliminary ligand docking studies indicated unfavorable interactions in the active site. As outlined in Scheme 3, nitration of 6-methyluracil (**11**) in the presence of H_2SO_4 and fuming nitric acid furnished 6-methyl-5-nitrouracil (**12**).[32] Condensation of compound **12** with aromatic aldehydes in the presence of piperidine provided the piperidine salts of 5-nitro-6-styryluracil derivatives **13**. The piperidine salts were neutralized by the addition of excess hydrochloric acid to give pure 5-nitro-6-styryluracil derivatives. The presence of the nitro group at the 5-position activates the methyl group for the reaction with piperidine acting as the basic catalyst.

The protocol did indeed seem to be versatile until the condensation was attempted with 2-nitrobenzaldehyde, 4-nitrobenzaldehyde, and 2,3-dihydroxybenzaldehyde. In those cases, the reaction did not produce the desired products, which is consistent with previous literature reports.[33] The protocol was therefore modified (Scheme 4) to provide the required 2-nitro derivative **14** and the other desired condensation products. Instead of using piperidine as the

(29) Grahner, B.; Winiwarter, S.; Lanzner, W.; Muller, C. E. *J. Med. Chem.* **1994**, *37*, 1526–1534.
(30) Nishigaki, S.; Kanamori, Y.; Senga, K. *Chem. Pharm. Bull.* **1980**, *28*, 1636–1641.
(31) Senga, K.; Ichiba, M.; Nishigaki, S. *J. Org. Chem.* **1979**, *44*, 3830–3834.
(32) Cresswell, R. M.; Wood, H. S. C. *J. Chem. Soc.* **1960**, 4768–4775.
(33) Ross, W. C. J. *J. Chem. Soc.* **1948**, 1128–1135.

solvent, which initially resulted in the piperidine salt of the condensation product, the reaction was performed in 1-butanol, a high-boiling alcohol, in the presence of 1 equiv of piperidine.

Two classes of compounds were synthesized as shown in structures **9**, **15**−**18** (class I), and **19**−**24** (class II). The enzyme-inhibitory activities of these compounds were determined using lumazine synthases from *M. tuberculosis* and *S. pombe* and riboflavin synthases from *Escherichia coli* and *M. tuberculosis*. The results are listed in Table 1.

Class I
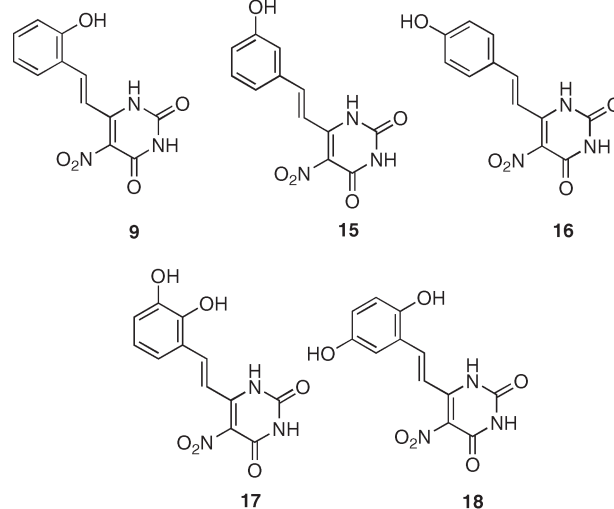
Class II
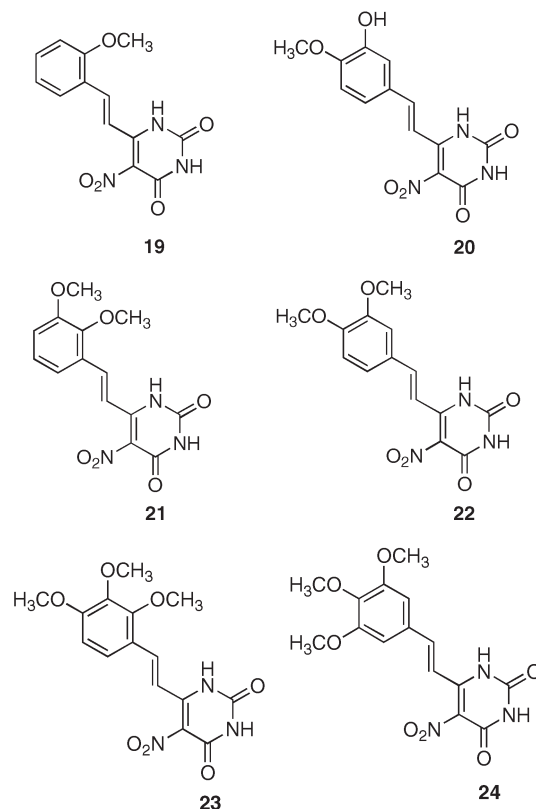
The hit compound **9** exhibits a K_i of 210 μM vs *S. pombe* lumazine synthase and a K_i of 95 μM vs *M. tuberculosis*

TABLE 1. Inhibition Constants vs *S. pombe* Lumazine Synthase, *M. tuberculosis* Lumazine Synthase, *M. tuberculosis* Riboflavin Synthase, *E. coli* Riboflavin Synthase[a]

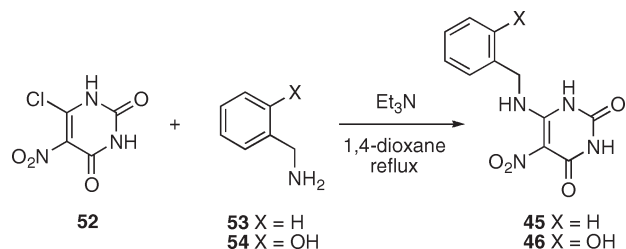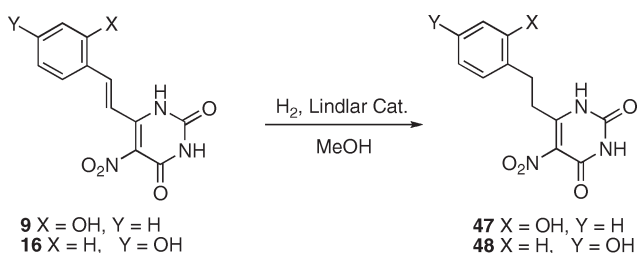| compd	enzyme	K_s,[b] μM	k_{cat},[c] min^{-1}	K_i,[d] μM	K_{is},[e] μM	mode of inhibition
9	*S. pombe* LS	2.0 ± 0.2	1.38 ± 0.03	210 ± 30		competitive
	M. tuberculosis LS	13 ± 1	0.26 ± 0.01	95 ± 6		competitive
	M. tuberculosis RS	63 ± 6	4.1 ± 0.2		917 ± 212	uncompetitive
14	*M. tuberculosis* LS	38 ± 3	0.31 ± 0.01	16 ± 3	49 ± 12	partial
15	*M. tuberculosis* LS	50 ± 7	0.23 ± 0.01	7.1 ± 0.8		competitive
16	*M. tuberculosis* LS	17 ± 2	0.43 ± 0.01	12 ± 5	17 ± 5	partial
17	*E. coli* RS	2.6 ± 0.3	5.1 ± 0.1	10 ± 3	26 ± 4	mixed
	S. pombe LS	1.2 ± 0.1	1.57 ± 0.02	4.9 ± 0.9	16 ± 3	partial
	M. tuberculosis LS	20 ± 2	0.36 ± 0.01	12 ± 4	81 ± 29	mixed
	M. tuberculosis RS	7.2 ± 1.0	0.27 ± 0.02	19 ± 9	37 ± 16	partial
18	*E. coli* RS	3.4 ± 0.3	5.1 ± 0.1		122 ± 10	uncompetitive
	S. pombe LS	2.5 ± 0.2	1.47 ± 0.04		53 ± 5	uncompetitive
	M. tuberculosis LS	22 ± 3	0.17 ± 0.01		420 ± 168	uncompetitive
	M. tuberculosis RS	7.7 ± 1.3	0.22 ± 0.02		398 ± 156	uncompetitive
19	*S. pombe* LS	1.03 ± 0.04	1.71 ± 0.01	205 ± 91	733 ± 227	mixed
	M. tuberculosis LS	6.4 ± 0.5	0.322 ± 0.004	28 ± 7	44 ± 10	partial
20	*S. pombe* LS	1.4 ± 0.1	1.41 ± 0.02		38 ± 2	uncompetitive
	M. tuberculosis LS	36 ± 3	0.28 ± 0.01	52 ± 19	74 ± 12	mixed
21	*S. pombe* LS	1.7 ± 0.1	2.21 ± 0.02	243 ± 57		competitive
	M. tuberculosis LS	31 ± 3	0.33 ± 0.01	9.6 ± 4.5	22 ± 6	mixed
22	*M. tuberculosis* LS	21 ± 2	0.33 ± 0.01	32 ± 16	32 ± 3	mixed
23	*M. tuberculosis* LS	34 ± 4	0.34 ± 0.01	48 ± 23	97 ± 24	mixed
24	*S. pombe* LS	1.2 ± 0.2	1.40 ± 0.03		47 ± 4	uncompetitive
	M. tuberculosis LS	37 ± 3	0.27 ± 0.01	17 ± 4	37 ± 5	mixed
25	*S. pombe* LS	1.1 ± 0.1	1.14 ± 0.02	42 ± 10	496 ± 219	mixed
	M. tuberculosis LS	6.0 ± 0.6	0.33 ± 0.01	11 ± 2	173 ± 50	mixed
26	*S. pombe* LS	0.85 ± 0.08	1.30 ± 0.02	13 ± 4	15 ± 5	partial
	M. tuberculosis LS	28 ± 3	0.45 ± 0.01	3.7 ± 0.9	37 ± 17	mixed
27	*S. pombe* LS	0.63 ± 0.08	1.39 ± 0.03	41 ± 18	187 ± 43	mixed
	M. tuberculosis LS	8.1 ± 0.5	0.353 ± 0.004	35 ± 10	78 ± 38	partial
28	*M. tuberculosis* LS	33 ± 4	0.27 ± 0.01	7.8 ± 4.6	13 ± 3	mixed
29	*M. tuberculosis* LS	36 ± 6	0.39 ± 0.02	86 ± 51	25 ± 8	mixed
	M. tuberculosis RS	14 ± 1	0.40 ± 0.01	361 ± 179	776 ± 294	mixed
30	*S. pombe* LS	0.62 ± 0.02	1.23 ± 0.01		604 ± 54	uncompetitive
	M. tuberculosis LS	7.2 ± 0.6	0.34 ± 0.01	26 ± 5	234 ± 59	mixed
31	*M. tuberculosis* LS	8.7 ± 0.7	0.37 ± 0.01	45 ± 13	188 ± 38	mixed
32	*M. tuberculosis* LS	26 ± 3	0.64 ± 0.03	31 ± 3		competitive
	M. tuberculosis RS	10 ± 0.5	0.47 ± 0.01		800 ± 107	uncompetitive
33	*M. tuberculosis* LS	21 ± 2	0.59 ± 0.02	42 ± 11	72 ± 19	partial
	M. tuberculosis RS	9.7 ± 0.4	0.45 ± 0.01		936 ± 138	uncompetitive
34	*S. pombe* LS	1.1 ± 0.1	1.09 ± 0.02	85 ± 39	682 ± 409	mixed
	M. tuberculosis LS	6.4 ± 0.6	0.38 ± 0.01	23 ± 5	225 ± 59	mixed
35	*E. coli* RS	3.0 ± 0.1	4.3 ± 0.1		224 ± 22	uncompetitive
	S. pombe LS	0.94 ± 0.06	1.13 ± 0.01	94 ± 34	497 ± 159	mixed
	M. tuberculosis LS	8.4 ± 0.6	0.38 ± 0.01	12 ± 1		competitive
36	*S. pombe* LS	0.72 ± 0.04	1.32 ± 0.01		276 ± 16	uncompetitive
	M. tuberculosis LS	7.9 ± 0.4	0.37 ± 0.01	87 ± 40	461 ± 150	mixed
37	*S. pombe* LS	0.85 ± 0.07	1.64 ± 0.02	130 ± 59	921 ± 640	mixed
	M. tuberculosis LS	6.7 ± 0.3	0.40 ± 0.01	197 ± 112	468 ± 113	mixed
38	*S. pombe* LS	0.93 ± 0.06	0.99 ± 0.01	151 ± 81	390 ± 90	mixed
	M. tuberculosis LS	6.4 ± 0.6	0.35 ± 0.01	24 ± 6	89 ± 11	mixed
39	*S. pombe* LS	4.3 ± 0.6	2.2 ± 0.1	143 ± 54		competitive
	M. tuberculosis LS	30 ± 4	4.3 ± 0.2	15 ± 7.3	15 ± 4	partial
40	*E. coli* RS	2.9 ± 0.2	3.6 ± 0.1	114 ± 44	806 ± 401	mixed
	S. pombe LS	0.83 ± 0.07	1.04 ± 0.01	13 ± 2	248 ± 67	mixed
	M. tuberculosis LS	7.6 ± 0.5	0.38 ± 0.01	30 ± 8	42 ± 12	partial
42	*M. tuberculosis* LS	19 ± 2	0.42 ± 0.01	26 ± 11	24 ± 10	partial
43	*E. coli* RS	2.2 ± 0.1	3.32 ± 0.05		270 ± 32	uncompetitive
	S. pombe LS	0.59 ± 0.03	2.58 ± 0.02	94 ± 30	476 ± 89	mixed
	M. tuberculosis LS	11 ± 1	0.37 ± 0.01	11 ± 3	72 ± 31	partial
44	*E. coli* RS	2.3 ± 0.1	3.40 ± 0.04		426 ± 64	uncompetitive
	S. pombe LS	1.2 ± 0.1	1.96 ± 0.04	141 ± 87	376 ± 127	mixed
	M. tuberculosis LS	7.8 ± 0.6	0.40 ± 0.01	70 ± 31	488 ± 233	mixed
45	*M. tuberculosis* LS	15 ± 1	0.56 ± 0.01		823 ± 128	uncompetitive
46	*M. tuberculosis* LS	18 ± 1	0.62 ± 0.02		904 ± 193	uncompetitive
48	*M. tuberculosis* RS	8.5 ± 0.4	0.34 ± 0.01		449 ± 45	uncompetitive
49	*S. pombe* LS	1.4 ± 0.1	1.12 ± 0.02		154 ± 13	uncompetitive
50	*E. coli* RS	2.7 ± 0.3	4.2 ± 0.1		788 ± 148	uncompetitive

[a]Experiments were conducted with recombinant lumazine synthases of *S. pombe* and *M. tuberculosis* and recombinant riboflavin synthases of *M. tuberculosis* and *E. coli*. The assays with lumazine synthase were performed with dihydroxybutanone phosphate substrate concentration held constant, while the concentration of the pyrimidinedione substrate was varied. [b]K_s is the substrate dissociation constant for the equilibrium E + S $\rightleftharpoons$ ES. [c]K_{cat} is the rate constant for the process ES $\rightarrow$ E + P. [d]K_i is the inhibitor dissociation constant for the process E + I $\rightleftharpoons$ EI. [e]K_{is} is the inhibitor dissociation constant process ES + I $\rightleftharpoons$ ESI. Partial and mixed modes of inhibition are similar, except the partial mode contains an additional product-formation step ESI $\rightarrow$ EI + P. Reaction mixtures contained 50 mM Tris·HCl, pH 7.0, 100 mM NaCl, and 5 mM DTT. The following compounds were inactive vs *M. tuberculosis* LS: **41, 47−51**; vs *S. pombe* LS: **14−16, 22, 23, 28, 29, 31, 41, 42, 50**; vs *M. tuberculosis* RS: **14−16, 19−28, 30, 31, 34−47, 49−51** and vs *E. coli* RS: **14−16, 19−31, 34, 36−39, 41, 42, 49**. The following compounds were not tested vs *S. pombe* LS: **32, 33, 45, 46, 48** and vs *E. coli* RS: **33, 45, 46, 48**.
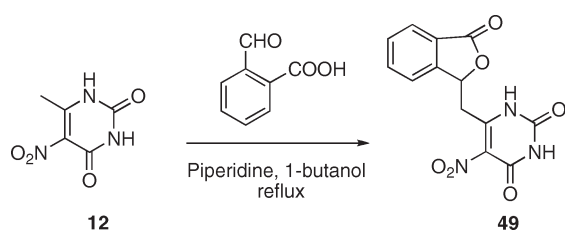
SCHEME 5

52   **53** X = H   **54** X = OH   →   **45** X = H   **46** X = OH

SCHEME 6

9 X = OH, Y = H   **16** X = H, Y = OH   →   **47** X = OH, Y = H   **48** X = H, Y = OH

SCHEME 7

12   →   **49**

lumazine synthase. To determine the effect of the position of the hydroxy group in the phenyl ring on the enzyme inhibitory activity, class I compounds were synthesized. Compound **15**, with a 3-hydroxy group, and compound **16**, with a 4-hydroxy group, showed marked increases in inhibitory activity, with the 3-hydroxy compound **15** exhibiting a K_i of 7.1 μM and 4-hydroxy compound **16** exhibiting a K_i 12 μM vs *M. tuberculosis* lumazine synthase. Both compounds **15** and **16** displayed remarkable selectivity for inhibition of *M. tuberculosis* lumazine synthase, being completely ineffective against *S. pombe* lumazine synthase and *E. coli* riboflavin synthase. Thus, changing the position of the phenol improved both the inhibitory activity vs *M. tuberculosis* lumazine synthase as well as the selectivity.

The presence of two hydroxyl groups on compounds **17** and **18** changed the inhibitory activity profile drastically. Both of these compounds were found to be potent against *M. tuberculosis* lumazine synthase, *M. tuberculosis* riboflavin synthase, *S. pombe* lumazine synthase, and *E. coli* riboflavin synthase, with compound **17** being more potent than compound **18**. Compound **17** exhibited a broader spectrum enzyme—inhibitory profile than the hit compound **9**, with a K_i of 12 μM vs *M. tuberculosis* lumazine synthase, a K_i of 19 μM vs *M. tuberculosis* riboflavin synthase, a K_i of 4.9 μM vs *S. pombe* lumazine synthase, and a K_i of 10 μM vs *E. coli* riboflavin synthase.

The hypothetical structural model of hit compound **9** in *M. tuberculosis* lumazine synthase (Figure 1) indicates that

the hydroxy group may hydrogen bond with the Ala59, Ile60, and Glu61 amino acid residues. Class II compounds were synthesized in order to determine the importance of hydrogen bond donor and acceptor properties. Class II compounds with OCH$_3$ groups displayed slightly better potencies than their counterparts with OH groups. Compound **21** exhibited a K_i of 9.6 μM vs *M. tuberculosis* lumazine synthase, whereas compound **17** showed a K_i of 12 μM vs *M. tuberculosis* lumazine synthase. Similarly, compound **19** exhibited a K_i of 28 μM vs *M. tuberculosis* lumazine synthase, whereas hit compound **9** displayed a K_i of 95 μM vs *M. tuberculosis* lumazine synthase.

In class III compounds, the hydroxyl groups have been replaced with different functional groups that can also participate in hydrogen bonding. Compounds with a NO$_2$ group showed a marked increase in inhibitory activity as compared to the lead compound **9**. Compound **14** exhibited a K_i of 16 μM vs *M. tuberculosis* lumazine synthase, whereas the hit compound **9** had a K_i of 95 μM vs *M. tuberculosis* lumazine synthase. The 4-NO$_2$ derivative **26** displayed the best inhibitory activity, with a K_i of 3.7 μM vs *M. tuberculosis* lumazine synthase. Among the compounds with different halogens, the 2-fluoro derivative **28** had the best activity with a K_i of 7.8 μM vs *M. tuberculosis* lumazine synthase. Thus, improved inhibitors of *M. tuberculosis* lumazine synthase were obtained by changing the OH group in the hit compound **9** to a NO$_2$ group or to F.

Class III

**14**   **25**   **26**

27   **28**   **29**

30   **31**
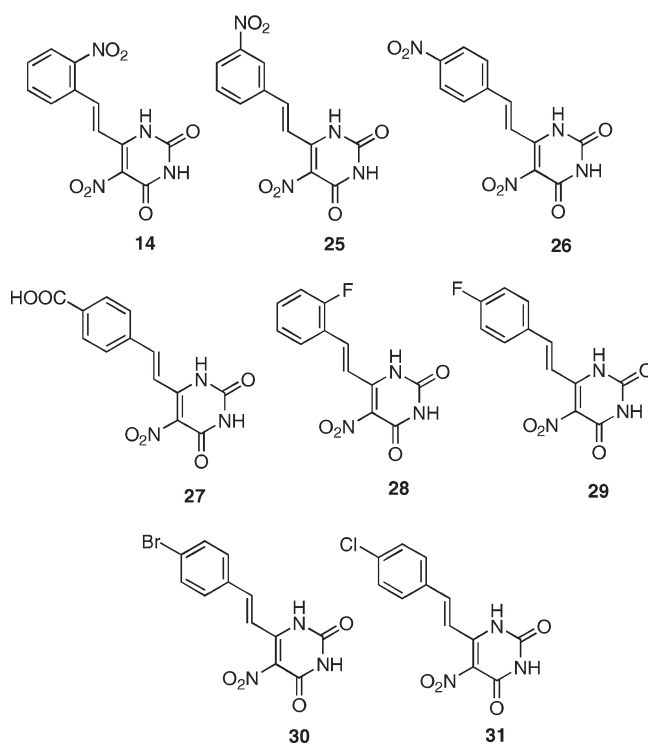
Classes I—III yielded two compounds **26** and **15** with optimized inhibitory activity. Based on these results, class IV compounds were designed with two different hydrogen bonding groups in the benzene ring. This may result in the

phenyl substituent more closely mimicking the ribityl chain of the substrate, with more opportunities for hydrogen bonding to the protein. These inhibitors were prepared following the standard protocol, with 1-butanol as the solvent and 1 equiv of piperidine as the base.

Class IV

32   33

34   35

36   37

38
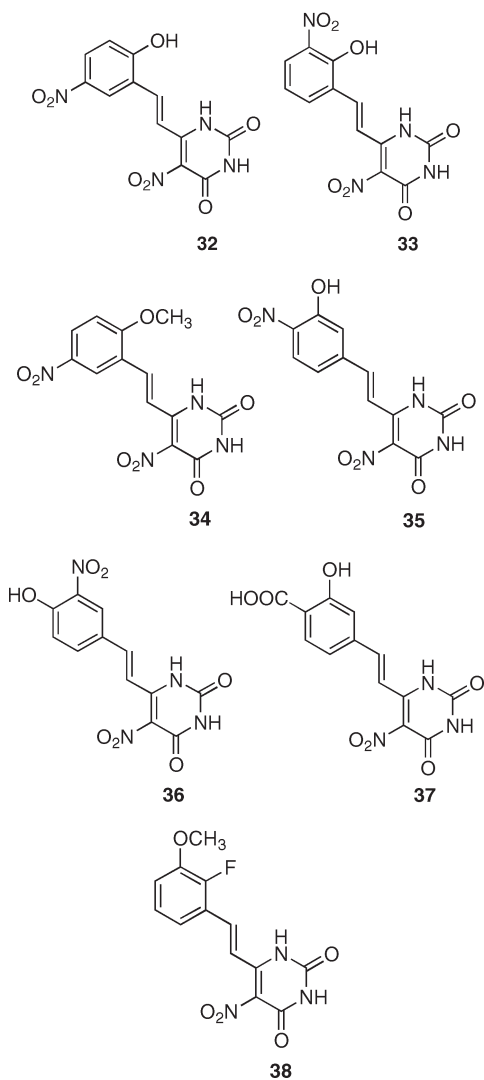
The enzyme inhibitory activities of the class IV compounds were disappointing. In fact, they had less inhibitory activity than their counterparts with single functional groups. Compound **35** showed the best inhibitory profile, with a K_i of 12 μM against *M. tuberculosis* lumazine synthase. These discouraging results prompted a reevaluation of the hypothesis that the functional groups on the aromatic ring hydrogen bond with the amino acid residues in the active site of *M. tuberculosis* lumazine synthase. This led to the synthesis of compounds **39** and **43** in the series of class V compounds, which contain unsubstituted aromatic rings. Compound **39** was expected to be a very weak inhibitor, but to the contrary, it was found to have good inhibitory activity, with a K_i of 15 μM vs *M. tuberculosis* lumazine synthase, which is much better than the hit compound **9** (K_i 95 μM vs *M. tuberculosis* lumazine synthase). Compound **43**, with a

naphthyl substituent, exhibited even better inhibitory activity, with a K_i of 11 μM vs *M. tuberculosis* lumazine synthase.

Class V

39   40   41

42   43   44
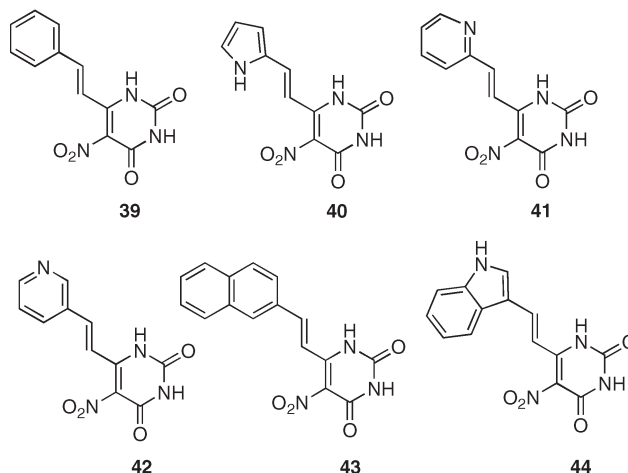
In Class VI compounds, the alkene linker is replaced by more flexible ethylene and aminomethylene connectors. The increase in conformational freedom should confer greater similarity with the substrate **1**.

Class VI

45   46   47

48   49

50   51
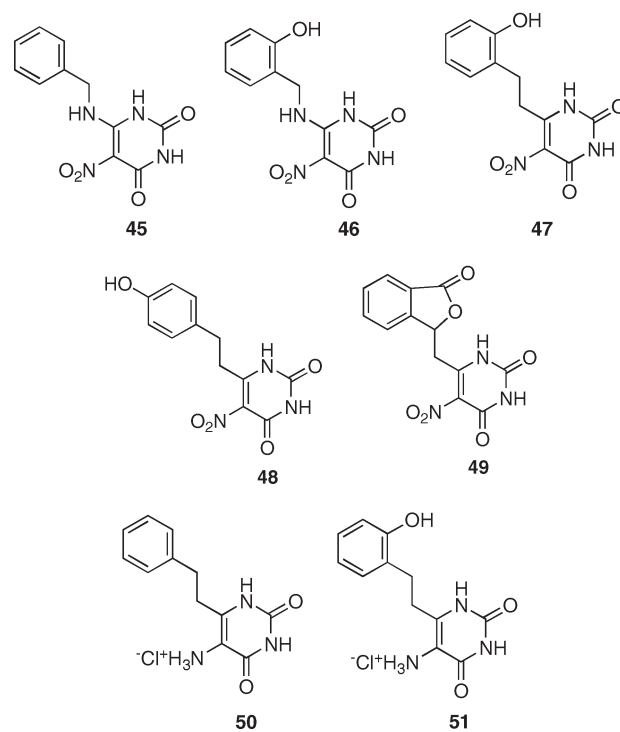
Compounds **45** and **46** were synthesized (Scheme 5) by treating 6-chloro-5-nitrouracil (**52**) with benzylamines **53** and **54** in the presence of triethylamine. The free bases were liberated from their triethylamine salts by dissolving them in aq KOH and neutralizing with dilute HCl solution.

Compounds **47** and **48** were prepared by selective reduction of the trans alkene linkers present in **9** and **16** (Scheme 6).

The presence of the reducible NO_2 group and conjugated double bond in compounds **9** and **16** made these alkenes difficult to selectively reduce. The usual protocol involving Pd/C reduced both the NO_2 group and the double bond. After unsuccessful attempts to selectively reduce either the double bond or the nitro group with Fe or Zn in acetic acid, Zn and hydrazinium monoformate, and $Na_2S_2O_4$, it was discovered that hydrogenation over Lindlar catalyst resulted in selective reduction of the alkene linker without reduction of the NO_2 group.

Compound **49** was accidentally formed during the condensation reaction of compound **12** with 2-formylbenzoic acid (Scheme 7). Evidently, the alcohol intermediate formed from **12** and 2-formylbenzoic acid lactonizes to **49** instead of dehydrating to the alkene. The structure of the lactone **49** suggests that 5-nitro-6-styryluracil derivatives might be susceptible to nucleophilic attack on the exocyclic double bond, but no instance of this was observed in the present series of compounds, which in general were quite stable.

The NO_2 group and the trans double bond in **9** and **39** were simultaneously reduced by hydrogenation using Pd/C to obtain compounds **50** and **51** (Scheme 8). This completes the synthesis of class VI compounds.

All compounds in class VI are either completely inactive or have very weak inhibitory activity. Molecular modeling was performed in order to investigate the possible bonding mode of compound **46** to the enzyme. The compound **46** was docked into the *M. tuberculosis* lumazine synthase structure using Gold software (BST, version 3.0, 2005). Energy minimization was then performed using Sybyl 7.1. The resulting structure is displayed in Figure 2. According to the theoretical model, the binding of the 2-hydroxyphenyl moiety of **46** in the active site of *M. tuberculosis* lumazine synthase is similar to the high-throughput screening compound **9**. However, the model indicates that the uracil ring of **46** does not stack with Trp 27, which may explain the inactivity of **45**−**48**.

In conclusion, high-throughput screening of a 100000 compound commercial library led to the identification of the hit compound **9**, which displayed a K_i of 95 μM vs *M. tuberculosis* lumazine synthase. The design and synthesis of a focused array of structural analogues provided the optimized congener **26**, which had a K_i of 3.7 μM vs *M. tuberculosis* lumazine synthase. Both of these compounds are structural analogs of the lumazine synthase substrate **1** and the known lumazine synthase ligand **10**. The results of this study show that the ribitylamino side chain of the ligand **10** can be replaced by substituted styryl moieties with retention of affinity for the enzyme. The circumvention of the ribitylamino side chain may contribute positively to antibiotic drug development because its polarity is expected to limit uptake by bacterial cells. As expected from the fact that the pyrimidinedione **1** is a substrate of the lumazine synthase-catalyzed reaction and a product of the riboflavin synthase-catalyzed reaction, many of the styryl derivatives in the present series, including **9**, **17**, **18**, **29**, **32**, **33**, **35**, **40**, **43**, **44**, **48**, and **50**, inhibited both enzymes. This is a potential advantage because drug resistance is less likely to emerge from target mutation with antibiotics that act on two targets, since resistance mutations would have to emerge in both targets at the same time for the organism to become drug resistant. Although it was previously demonstrated that the intermediate analogue **55**, in which the ribityl group is

SCHEME 8

9 X = OH
39 X = H

51 X = OH
50 X = H
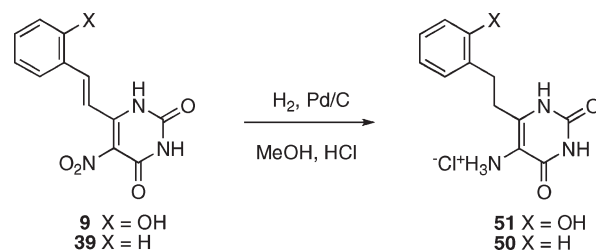
replaced by a chlorine atom, has affinity for lumazine synthase, compound **55** also has a phosphate moiety that contributes positively to binding.[27] It therefore contrasts with the present series of inhibitors, which do not contain a phosphate moiety.

55
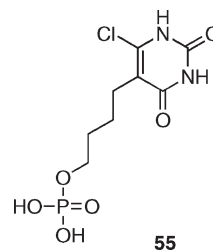
Experimental Section

General Procedure: Method A. 5-Nitro-6-methyluracil (**12**) (1.0 g, 5.85 mmol), benzaldehyde derivatives (29.2 mmol), and piperidine (10 mL) were heated at first on a boiling water bath until the mixture had thickened and then for 30 min in an oil bath at 150 °C. The mixture was diluted with methanol (15 mL), and the crystalline solid was filtered, washed with methanol (5 mL) and ether (10 mL), and dried to give the piperidine salt. The salt was dissolved in dilute KOH solution. On the addition of excess of hydrochloric acid to the warm solution, a yellow powder precipitated. This was filtered and washed first with water (2 × 10 mL) and methanol (2 × 10 mL) and then with ether (2 × 10 mL) to give the desired condensation product.

(E)-6-(3-Hydroxystyryl)-5-nitropyrimidine-2,4(1H,3H)-dione (15). A yellow amorphous solid **15** (1.20 g, 75%): mp 238−240 °C dec; ^{1}H NMR (300 MHz, CDCl$_3$) δ 7.53 (d, J = 16.4 Hz, 1 H), 7.16 (t, J = 7.8 Hz, 1 H), 6.97 (d, J = 7.6 Hz, 1 H), 6.92 (s, 1 H), 6.86 (d, J = 16.4 Hz, 1 H), 6.77 (d, J = 8.1 Hz, 1 H); ^{13}C NMR (75 MHz, DMSO-d_6) δ 158.0, 156.9, 149.4, 147.8, 142.3, 135.8, 130.5, 126.7, 119.7, 118.3, 114.4, 113.8; EIMS m/z 275 (M$^+$). Anal. Calcd for C$_{12}$H$_9$N$_3$O$_5$: C, 52.37; H, 3.30; N, 15.27. Found: C, 52.58; H, 3.14; N, 15.54.

(E)-6-(4-Hydroxystyryl)-5-nitropyrimidine-2,4(1H,3H)-dione (16). An orange amorphous solid **16** (1.25 g, 78%): mp 230−232 °C dec; ^{1}H NMR (300 MHz, CDCl$_3$) δ 7.64 (d, J = 16.3 Hz, 1 H), 7.52 (d, J = 8.64 Hz, 2 H), 6.87 (J = 8.64 Hz, 2 H), 6.85 (d, J = 16.3 Hz, 1 H); ^{13}C NMR (75 MHz, DMSO-d_6) δ 160.6, 156.9, 149.5, 148.0, 142.7, 130.8, 126.1, 125.7, 116.3, 109.9; negative-ion EIMS m/z 549 [(2 M−H$^+$)$^-$, 100], 275 (M, 11), 274 [(M−H$^+$)$^-$, 98], 144 (4). Anal. Calcd for C$_{12}$H$_9$N$_3$O$_5$: C, 52.37; H, 3.30; N, 15.27. Found: C, 52.45; H, 3.24; N, 15.58.

(E)-6-(3-Hydroxy-4-methoxystyryl)-5-nitropyrimidine-2,4(1H,3H)-dione (20). A red amorphous solid **20** (625 mg, 67%): mp 300−304 °C; ^{1}H NMR (300 MHz, DMSO-d_6) δ 9.34 (s, 1 H), 7.68 (d, J = 16.2 Hz, 1 H), 7.06 (s, 1 H), 7.04 (d, J = 7.8 Hz, 1 H), 6.98 (d, J = 7.8 Hz, 1 H), 6.69 (d, J = 16.2 Hz, 1 H), 3.81 (s, 3 H); ^{13}C NMR (75 MHz, DMSO-d_6) δ 156.8, 150.7, 149.4, 147.8, 147.0, 142.5, 127.1, 126.0, 121.8, 113.9, 112.2, 110.7, 55.7; negative-ion EIMS

FIGURE 2. Hypothetical model showing hydrogen bonding between the phenolic hydroxyl group of compound **46** with Ala59 and Glu61 of *M. tuberculosis* lumazine synthase. The distances shown are in Å. The diagram is programmed for wall-eyed (relaxed) viewing.

m/z 609 [(2 M − H$^+$)$^-$, 46], 304 [(M − H$^+$)$^-$, 100]. Anal. Calcd for C$_{13}$H$_{11}$N$_3$O$_6$: C, 51.15; H, 3.63; N, 13.77. Found: C, 50.80; H, 3.80, N, 13.43.

(*E*)-6-(2,3-Dimethoxystyryl)-5-nitropyrimidine-2,4(1*H*,3*H*)-dione (21). An orange, amorphous solid **21** (655 mg, 70%): mp 280−283 °C; ^{1}H NMR (300 MHz, DMSO-d_6) δ 7.25 (d, J = 16.5 Hz, 1 H), 6.57 (m, 1 H), 6.48 (m, 1 H), 6.36 (d, J = 16.2 Hz, 1 H), 3.18 (s, 3 H), 3.14 (s, 3 H); ^{13}C NMR (75 MHz, DMSO-d_6) δ 157.1, 153.3, 149.8, 148.5, 148.1, 137.1, 128.4, 127.0, 124.9, 119.6, 115.5, 115.3, 61.2, 56.0; negative-ion EIMS m/z 637 [(2 M − H$^+$)$^-$, 100], 318 [(M − H$^+$)$^-$, 46]. Anal. Calcd for C$_{14}$H$_{13}$N$_3$O$_6$·0.5H$_2$O: C, 51.22; H, 4.30; N, 12.80. Found: C, 51.03; H, 3.91, N, 12.53.

(*E*)-6-(3,4-Dimethoxystyryl)-5-nitropyrimidine-2,4(1*H*,3*H*)-dione (22). A red amorphous solid **22** (625 mg, 67%): mp 328−230 °C; ^{1}H NMR (300 MHz, DMSO-d_6) δ 7.67 (d, J = 16.2 Hz, 1 H), 7.23 (d, J = 1.6 Hz, 1 H), 7.16 (dd, J = 1.6 Hz, 8.4 Hz, 1 H), 7.00 (d, J = 8.4 Hz, 1 H), 6.85 (d, J = 16.2 Hz, 1 H), 3.80 (s, 3 H), 3.77 (s, 3 H); ^{13}C NMR (75 MHz, DMSO-d_6) δ 156.7, 151.5, 149.4, 149.1, 147.9, 142.3, 127.1, 126.0, 123.5, 111.7, 111.3, 110.0, 55.7; negative-ion EIMS m/z 637 [(2 M − H$^+$)$^-$, 14], 318 [(M − H$^+$)$^-$, 100]. Anal. Calcd for C$_{14}$H$_{13}$N$_3$O$_6$: C, 52.67; H, 4.10; N, 13.16. Found: C, 52.69; H, 3.87, N, 13.01.

(*E*)-6-(2,3,4-Trimethoxystyryl)-5-nitropyrimidine-2,4(1*H*,3*H*)-dione (23). A red amorphous solid **23** (610 mg, 60%): mp 308−310 °C; ^{1}H NMR (300 MHz, DMSO-d_6) δ 7.81 (d, J = 16.8 Hz, 1 H), 7.39 (d, J = 9.5 Hz, 1 H), 6.95 (d, J = 16.8 Hz, 1 H), 6.88 (d, J = 9.5 Hz, 1 H), 3.88 (s, 3 H), 3.86 (s, 3 H), 3.79 (s, 3 H); ^{13}C NMR (75 MHz, DMSO-d_6) δ 157.6, 155.6, 152.8, 149.4, 149.1, 141.9, 137.1, 126.1, 124.0, 120.7, 112.7, 108.3, 61.4, 60.6, 56.1; negative-ion EIMS m/z 697 [(2 M−H$^+$)$^-$, 100], 348 [(M − H$^+$)$^-$, 57]. Anal. Calcd for C$_{15}$H$_{15}$N$_3$O$_7$: C, 51.58; H, 4.33; N, 12.03. Found: C, 51.49; H, 4.35, N, 11.75.

(*E*)-6-(3,4,5-Trimethoxystyryl)-5-nitropyrimidine-2,4(1*H*,3*H*)-dione (24). A red amorphous solid **24** (610 mg, 60%): mp 293−296 °C dec; ^{1}H NMR (300 MHz, DMSO-d_6) δ 7.56 (d, J = 16.2 Hz, 1 H), 6.94 (d, J = 16.2 Hz, 1 H), 6.92 (s, 2 H), 3.76 (s, 3 H), 3.67 (s, 6 H); negative-ion EIMS m/z 697 [(2 M−H$^+$)$^-$, 43], 348 [(M − H$^+$)$^-$, 100]. Anal. Calcd for C$_{15}$H$_{15}$N$_3$O$_7$·1.25H$_2$O: C, 48.46; H, 4.74; N, 11.30. Found: C, 48.27; H, 4.71, N, 11.09.

(*E*)-6-(2-Fluorostyryl)-5-nitropyrimidine-2,4(1*H*,3*H*)-dione (28). An orange, amorphous solid **28** (510 mg, 63%): mp 280−283 °C dec; ^{1}H NMR (300 MHz, MeOH-d_4) δ 7.82 (d, J = 16.5 Hz, 1 H), 7.78 (m, 1 H), 7.50 (m, 1 H), 7.33 (d, J = 8.9 Hz, 1 H), 7.27 (d, J = 7.1 Hz, 1 H), 7.07 (d, J = 16.5 Hz, 1 H); ^{13}C NMR (75 MHz, MeOH-d_4) δ 162.5, 156.6, 149.3, 147.5, 133.8, 132.8, 129.1, 126.6, 125.2, 116.6, 116.5. Anal. Calcd for C$_{12}$H$_8$FN$_3$O$_4$: C, 51.99; H, 2.91; N, 15.16. Found: C, 51.79; H, 3.05, N, 15.25.

(*E*)-6-(4-Fluorostyryl)-5-nitropyrimidine-2,4(1*H*,3*H*)-dione (29). A red amorphous solid **29** (488 mg, 60%): mp 286−288 °C; ^{1}H NMR (300 MHz, MeOH-d_4) δ 7.73 (d, J = 16.0 Hz, 1 H), 7.45 (d, J = 8.3 Hz, 2 H), 6.94 (d, J = 8.4 Hz, 2 H), 6.66 (d, J = 16.0 Hz, 1

H); ^{13}C NMR (75 MHz, MeOH-d_4) δ 156.7, 152.7, 149.3, 147.9, 142.7, 130.3, 125.3, 122.8, 114.2, 107.6; negative-ion EIMS m/z (rel intensity) 276 [(2 M − H$^+$)$^-$, 100], 113 (2). Anal. Calcd for C$_{12}$H$_8$FN$_3$O$_4$·0.1H$_2$O: C, 51.66; H, 2.96; N, 15.06. Found: C, 51.95; H, 3.22, N, 14.69.

5-Nitro-6-styryluracil (39). A yellow amorphous solid **39** (5.1 g, 84%): mp 308−310 °C (lit.[33] mp 312−314 °C); ^{1}H NMR (300 MHz, MeOH-d_4) δ 7.78 (d, J = 16.2 Hz, 1 H), 7.63 (m, 2 H), 7.44 (m, 3 H), 6.98 (d, J = 16.2 Hz, 1 H); ^{13}C NMR (75 MHz, MeOH-d_4) δ 157.0, 149.6, 147.2, 134.6, 131.1, 129.5, 128.6, 126.8, 114.2; negative-ion EIMS m/z 259 (M, 12), 258 [(M−H$^+$)$^-$, 98.5], 113 (2). Anal. Calcd for C$_{12}$H$_9$N$_3$O$_4$: C, 55.60; H, 3.50; N, 16.21. Found: C, 55.89; H, 3.41; N, 15.95.

(*E*)-5-Nitro-6-(2-(pyridin-2-yl)vinyl)pyrimidine-2,4(1*H*,3*H*)-dione (41). An orange amorphous solid **41** (1.29 g, 85%): mp 290−292 °C dec; ^{1}H NMR (300 MHz, CDCl$_3$) δ 8.63 (d, J = 4.8 Hz, 1 H), 7.92 (t, J = 8.6 Hz, 1 H), 7.73 (d, J = 15.9 Hz, 1 H), 7.60 (d, J = 7.8 Hz, 1 H), 7.44 (d, J = 15.9 Hz, 1 H), 7.43 (m, 1 H); ^{13}C NMR (75 MHz, DMSO-d_6) δ 157.2, 150.6, 149.2, 148.3, 147.2, 141.3, 137.7, 128.0, 126.5, 126.4, 120.4; negative-ion EIMS m/z 541 [(2 MNa − 2H$^+$)$^-$, 100], 259 [(M − H$^+$)$^-$, 41]. Anal. Calcd for C$_{11}$H$_8$N$_4$O$_4$: C, 50.77; H, 3.10; N, 21.53. Found: C, 50.52; H, 3.16; N, 21.20.

(*E*)-5-Nitro-6-(3-(pyridin-3-yl)vinyl)pyrimidine-2,4(1*H*,3*H*)-dione (42). A yellow amorphous solid **42** (1.22 g, 80%): mp 300−303 °C; ^{1}H NMR (300 MHz, CDCl$_3$) δ 8.76 (s, 1 H), 8.59 (d, J = 3.7 Hz, 1 H), 8.13 (d, J = 8.07 Hz, 1 H), 7.70 (d, J = 16.2 Hz, 1 H), 7.46 (dd, J = 4.8 Hz, 7.8 Hz, 1 H), 7.19 (d, J = 16.2 Hz, 1 H); ^{13}C NMR (75 MHz, DMSO-d_6) δ 156.8, 151.03, 150.0, 149.8, 148.6, 137.8, 134.4, 130.3, 126.5, 124.2, 117.2; negative-ion EIMS m/z 556.8 [(2 M − 2H$^+$)$^-$, 100], 259 [(M − H$^+$)$^-$, 94], 156 (1). Anal. Calcd for C$_{11}$H$_8$N$_4$O$_4$: C, 50.77; H, 3.10; N, 21.53. Found: C, 50.47; H, 2.88; N, 21.71.

General Procedure: Method B. 5-Nitro-6-methyluracil (**12**) (0.5 g, 2.92 mmol), benzaldehyde derivatives (5.84 mmol), and piperidine (0.3 mL, 3.21 mmol) in 1-butanol (10 mL) were heated at first to 100 °C until the mixture had thickened and then at reflux for 6 h. The mixture was cooled to room temperature, filtered, and washed with methanol (5 mL) and ether (10 mL). The salt was dissolved in dilute KOH solution and acidified with an excess of hydrochloric acid, and the solid was filtered, washed with water (2 × 10 mL) and methanol (2 × 10 mL) and then with ether (2 × 10 mL), and dried to give the desired condensation product.

(*E*)-6-(2-Nitrostyryl)-5-nitropyrimidine-2,4(1*H*,3*H*)-dione (14). A brown amorphous solid **14** (0.62 mg, 69%): mp 298−300 °C; ^{1}H NMR (300 MHz, DMSO-d_6) δ 8.03 (d, J = 8.1 Hz, 1 H), 7.97 (d, J = 9.0 Hz, 1 H), 7.95 (d, J = 16.2 Hz, 1 H), 7.79 (t, J = 7.5 Hz, 1 H), 7.68 (d, J = 7.5 Hz, 1 H), 7.05 (d, J = 16.2 Hz, 1 H); ^{13}C NMR (75 MHz, DMSO-d_6) δ 156.9, 149.3, 148.8, 147.0, 135.6, 134.0, 131.3, 129.2, 128.9, 127.0, 125.0, 119.3; negative-ion

EIMS m/z (rel intensity) 607 [(2 M − H$^+$)$^−$, 100], 303 [(M − H$^+$)$^−$, 80], 240 (10). Anal. Calcd for C$_{12}$H$_8$N$_4$O$_6$: C, 47.38; H, 2.65; N, 18.42. Found: C, 47.45; H, 2.45; N, 18.10.

(*E*)-6-(2,3-Dihydroxystyryl)-5-nitropyrimidine-2,4(1*H*,3*H*)-dione (17). A brown amorphous solid 17 (0.49 g, 58%): mp 287−290 °C dec; ^{1}H NMR (300 MHz, DMSO-d_6) δ 7.88 (d, *J* = 15.7 Hz, 1 H), 7.07 (d, *J* = 15.7 Hz, 1 H), 6.85 (m, 2 H), 6.67 (t, *J* = 7.8 Hz, 1 H); ^{13}C NMR (75 MHz, DMSO-d_6) δ 156.1, 150.0, 149.5, 148.8, 147.4, 138.3, 125.4, 120.7, 119.3, 116.9, 114.2, 112.8; negative-ion EIMS m/z 581 [(2 M − H$^+$)$^−$, 62], 290 [(M − H$^+$)$^−$, 100]. Anal. Calcd for C$_{12}$H$_9$N$_3$O$_6$: C, 49.49; H, 3.12; N, 14.43. Found: C, 49.61; H, 3.22; N, 14.48.

(*E*)-6-(2,5-Dihydroxystyryl)-5-nitropyrimidine-2,4(1*H*,3*H*)-dione (18). A brown amorphous solid 18 (0.19 g, 23%): mp 279−282 °C dec; ^{1}H NMR (300 MHz, DMSO-d_6) δ 9.78 (brs, 1 H), 7.80 (d, *J* = 15.8 Hz, 1 H), 7.04 (d, *J* = 15.8 Hz, 1 H), 6.81 (d, *J* = 1.97 Hz, 1 H), 6.70 (m, 2 H); ^{13}C NMR (75 MHz, DMSO-d_6) δ 156.3, 149.9, 149.5, 148.9, 147.4, 138.5, 125.5, 120.7, 119.3, 116.7, 114.2, 112.7; negative-ion EIMS m/z (rel intensity) 581 [(2 M − H$^+$)$^−$, 100], 290 [(M − H$^+$)$^−$, 54], 244 (1). Anal. Calcd for C$_{12}$H$_9$N$_3$O$_6$: C, 49.49; H, 3.12; N, 14.43. Found: C, 49.78; H, 3.14; N, 14.29.

(*E*)-6-(2-Methoxystyryl)-5-nitropyrimidine-2,4(1*H*,3*H*)-dione (19). A yellow amorphous solid 19 (0.56 g, 66%): mp 289−300 °C; ^{1}H NMR (300 MHz, DMSO-d_6) δ 7.90 (d, *J* = 16.4 Hz, 1 H), 7.57 (d, *J* = 7.6 Hz, 1 H), 7.42 (t, *J* = 7.6 Hz, 1 H), 7.09 (d, *J* = 7.6 Hz, 1 H), 7.08 (d, *J* = 16.4 Hz, 1 H), 7.00 (d, *J* = 7.6 Hz, 1 H); ^{13}C NMR (75 MHz, DMSO-d_6) δ 158.3, 156.8, 149.5, 148.1, 137.6, 132.4, 129.5, 126.4, 122.8, 121.0, 114.6, 112.0, 55.8; negative-ion EIMS m/z 577 [(2 M − H$^+$)$^−$, 100], 288 [(M − H$^+$)$^−$, 58]. Anal. Calcd for C$_{13}$H$_{11}$N$_3$O$_5$: C, 53.98; H, 3.83; N, 14.53. Found: C, 53.92; H, 3.92; N, 14.17.

(*E*)-5-Nitro-6-(3-nitrostyryl)pyrimidine-2,4(1*H*,3*H*)-dione (25). A yellow amorphous solid 25 (0.56 g, 63%): mp 278−280 °C; ^{1}H NMR (300 MHz, DMSO-d_6) δ 8.44 (s, 1 H), 8.23 (dd, *J* = 1.44 Hz, 8.06 Hz, 1 H), 8.06 (d, *J* = 7.7 Hz, 1 H), 7.76 (d, *J* = 16.3 Hz, 1 H), 7.70 (d, *J* = 8.06 Hz, 1 H), 7.25 (d, *J* = 16.3 Hz, 1 H); ^{13}C NMR (75 MHz, DMSO-d_6) δ 156.6, 149.5, 148.3, 147.8, 138.9, 136.0, 134.3, 130.6, 126.8, 124.7, 122.5, 117.7; negative-ion EIMS m/z 607 [(2 M − H$^+$)$^−$, 100], 303 [(M − H$^+$)$^−$, 37]. Anal. Calcd for C$_{12}$H$_8$N$_4$O$_6$: C, 47.38; H, 2.65; N, 18.42. Found: C, 47.02; H, 2.73; N, 18.13.

(*E*)-5-Nitro-6-(4-nitrostyryl)pyrimidine-2,4(1*H*,3*H*)-dione (26). A brown amorphous solid 26 (0.62 mg, 69%): mp 304−308 °C dec; ^{1}H NMR (300 MHz, DMSO-d_6) δ 8.23 (d, *J* = 8.8 Hz, 2 H), 7.89 (d, *J* = 8.8 Hz, 2 H), 7.68 (d, *J* = 15.8 Hz, 1 H), 7.38 (d, *J* = 15.8 Hz, 1 H); ^{13}C NMR (75 MHz, DMSO-d_6) δ 156.7, 149.3, 148.1, 147.6, 140.6, 138.9, 129.3, 127.0, 124.3, 118.7. Anal. Calcd for C$_{12}$H$_8$N$_4$O$_6$: C, 47.38; H, 2.65; N, 18.42. Found: C, 47.52; H, 2.70; N, 18.19.

(*E*)-4-(2-(5-Nitro-2,6-dioxo-1,2,3,6-tetrahydropyrimidine-4-yl)vinyl)benzoic Acid (27). A pale-yellow amorphous solid 27 (0.28 mg, 64%): mp 342−345 °C; ^{1}H NMR (300 MHz, DMSO-d_6) δ 11.83 (brs, 1 H), 7.98 (brs, 1 H), 7.95 (brs, 1 H), 7.72 (d, *J* = 16.3 Hz, 1 H), 7.71 (m, 2 H), 7.07 (d, *J* = 16.3 Hz, 1 H); ^{13}C NMR (75 MHz, DMSO-d_6) δ 167.2, 156.8, 149.9, 147.7, 140.8, 138.2, 130.4, 128.2, 127.0, 116.8; negative-ion EIMS m/z 605 [(2 M − H$^+$)$^−$, 100], 302 [(M − H$^+$)$^−$, 70]. Anal. Calcd for C$_{13}$H$_9$N$_3$O$_6$·0.5H$_2$O: C, 50.01; H, 3.23; N, 13.46. Found: C, 50.29; H, 2.89; N, 13.22.

(*E*)-5-Nitro-6-(4-bromostyryl)pyrimidine-2,4(1*H*,3*H*)-dione (30). A yellow amorphous solid 30 (0.62 g, 63%): mp 296−298 °C dec; ^{1}H NMR (300 MHz, DMSO-d_6) δ 7.68 (d, *J* = 16.3 Hz, 1 H), 7.62 (dd, *J* = 8.4 Hz, 18.0 Hz, 4 H), 7.03 (d, *J* = 16.3 Hz, 1 H); ^{13}C NMR (75 MHz, DMSO-d_6) δ 156.7, 149.4, 147.7, 140.4, 133.5, 132.2, 130.2, 126.6, 124.2, 115.1. Anal. Calcd for C$_{12}$H$_8$BrN$_3$O$_4$: C, 42.63; H, 2.38; N, 12.43; Br, 23.63. Found: C, 42.41; H, 2.37; N, 12.27; Br, 23.55.

(*E*)-6-(4-Chlorostyryl)-5-nitropyrimidine-2,4(1*H*,3*H*)-dione (31). A yellow amorphous solid 31 (0.58 g, 67%): mp 326−328 °C;

^{1}H NMR (300 MHz, DMSO-d_6) δ 7.68 (d, *J* = 16.2 Hz, 1 H), 7.60 (d, *J* = 8.4 Hz, 2 H), 7.51 (d, *J* = 8.4 Hz, 2 H), 7.03 (d, *J* = 16.3 Hz, 1 H); ^{13}C NMR (75 MHz, DMSO-d_6) δ 156.7, 149.6, 148.1, 140.0, 135.2, 133.3, 130.0, 129.2, 115.4. Anal. Calcd for C$_{12}$H$_8$ClN$_3$O$_4$: C, 49.08; H, 2.75; Cl, 12.07; N, 14.35. Found: C, 48.89; H, 2.79; Cl, 11.89; N, 13.92.

(*E*)-6-(2-Hydroxy-5-nitrostyryl)-5-nitropyrimidine-2,4(1*H*,3*H*)-dione (32). A brick-red amorphous solid 32 (625 mg, 67%): mp 298−300 °C; ^{1}H NMR (300 MHz, DMSO-d_6) δ 11.83 (brs, 2 H), 8.38 (d, *J* = 2.8 Hz, 1 H), 8.14 (dd, *J* = 2.8, 9.0 Hz, 1 H), 7.83 (d, *J* = 16.4 Hz, 1 H), 7.34 (d, *J* = 16.4 Hz, 1 H), 7.07 (d, *J* = 9.0 Hz, 1 H); ^{13}C NMR (75 MHz, DMSO-d_6) δ 162.8, 156.8, 149.3, 147.8, 138.9, 136.2, 127.1, 126.8, 126.0, 121.7, 156.9, 156.8; negative-ion EIMS m/z (rel intensity) 639 [2 M − H$^+$)$^−$, 80], 319 [(M − H$^+$)$^−$, 100]. Anal. Calcd for C$_{12}$H$_8$N$_4$O$_7$·0.75H$_2$O: C, 43.19; H, 2.87; N, 16.79. Found: C, 43.38; H, 2.81; N, 16.68.

(*E*)-6-(2-Hydroxy-3-nitrostyryl)-3-nitropyrimidine-2,4(1*H*,3*H*)-dione (33). A yellowish-brown amorphous solid 33 (705 mg, 75%): mp 305−307 °C; ^{1}H NMR (300 MHz, DMSO-d_6) δ 8.04 (dd, *J* = 2.8 Hz, 1 H), 7.97 (d, *J* = 7.8 Hz, 1 H), 7.90 (d, *J* = 16.4 Hz, 1 H), 7.24 (d, *J* = 16.4 Hz, 1 H), 7.09 (t, *J* = 8.0 Hz, 1 H); EIMS m/z (rel intensity) 321 (MH$^+$, 32), 359 (MK$^+$, 50), 659 (100); negative-ion EIMS m/z (rel intensity) 319 [(M − H$^+$)$^−$, 100], 256 (11). Anal. Calcd for C$_{12}$H$_8$N$_4$O$_7$: C, 45.01; H, 2.52; N, 17.50. Found: C, 45.34; H, 2.55; N, 17.56.

(*E*)-6-(2-Methoxy-5-nitrostyryl)-5-nitropyrimidine-2,4(1*H*,3*H*)-dione (34). A yellow amorphous solid 34 (630 mg, 65%): mp 278−280 °C; ^{1}H NMR (300 MHz, DMSO-d_6) δ 11.88 (s, 1 H), 11.73 (s, 1 H), 8.46 (d, *J* = 2.6 Hz, 1 H), 8.29 (dd, *J* = 2.6, 9.2 Hz, 1 H), 7.84 (d, *J* = 16.4 Hz, 1 H), 7.33 (d, *J* = 9.2 Hz, 1 H), 7.27 (d, *J* = 16.4 Hz, 1 H); ^{13}C NMR (75 MHz, DMSO-d_6) δ 162.9, 156.7, 149.2, 147.8, 141.0, 134.9, 127.3, 126.8, 124.6, 123.5, 117.9, 112.9, 57.0; negative-ion EIMS m/z 667 [(2 M − H$^+$)$^−$, 100], 333 [(M − H$^+$)$^−$, 23]. Anal. Calcd for C$_{13}$H$_{10}$N$_4$O$_7$·0.5-H$_2$O: C, 45.49; H, 3.23; N, 16.32. Found: C, 45.31; H, 3.04; N, 16.20.

(*E*)-6-(3-Hydroxy-4-nitrostyryl)-5-nitropyrimidine-2,4(1*H*,3*H*)-dione (35). A pale yellow amorphous solid 35 (323 mg, 69%): mp 310−312 °C; ^{1}H NMR (300 MHz, DMSO-d_6) δ 11.73 (brs, 1 H), 11.19 (brs, 1 H), 7.94 (d, *J* = 8.6 Hz, 1 H), 7.66 (d, *J* = 16.3 Hz, 1 H), 7.30 (s, 1 H), 7.26 (d, *J* = 8.6 Hz, 1 H), 7.07 (d, *J* = 16.4 Hz, 1 H); ^{13}C NMR (75 MHz, DMSO-d_6) δ 156.6, 152.3, 149.2, 147.2, 140.5, 139.1, 137.3, 127.0, 126.1, 118.6, 118.5, 118.1; negative-ion EIMS m/z 639 [(2 M − H$^+$)$^−$, 100], 319 [(M − H$^+$)$^−$, 78]. Anal. Calcd for C$_{12}$H$_8$N$_4$O$_7$: C, 45.01; H, 2.52; N, 17.50. Found: C, 44.98; H, 2.54; N, 17.45.

(*E*)-6-(4-Hydroxy-3-nitrostyryl)-5-nitropyrimidine-2,4(1*H*,3*H*)-dione (36). A yellow amorphous solid 36 (315 mg, 67%): mp 320−322 °C. ^{1}H NMR (300 MHz, DMSO-d_6) δ 11.83 (s, 1 H), 11.55 (brs, 1 H), 8.12 (d, *J* = 1.9 Hz, 1 H), 7.78 (dd, *J* = 1.9, 8.7 Hz, 1 H), 7.67 (d, *J* = 16.3 Hz, 1 H), 7.15 (d, *J* = 8.7 Hz, 1 H), 6.92 (d, *J* = 16.3 Hz, 1 H); ^{13}C NMR (75 MHz, DMSO-d_6) δ 156.7, 153.8, 149.4, 147.5, 139.8, 137.4, 134.3, 126.4, 125.7, 125.4, 119.9; Pos EIMS m/z (rel intensity) 321 (M$^+$, 100); negative-ion EIMS m/z 639 [(2 M − H$^+$)$^−$, 100], 319 [(M − H$^+$)$^−$, 30]. Anal. Calcd for C$_{12}$H$_8$N$_4$O$_7$: C, 45.01; H, 2.52; N, 17.50. Found: C, 44.70; H, 2.58; N, 17.44.

(*E*)-3-Hydroxy-4-(2-(5-nitro-2,6-dioxo-1,2,3,6-tetrahydropyrimidine-4-yl)vinyl)benzoic Acid (37). A yellow red amorphous solid 37 (0.28 g, 60%): mp 347−349 °C dec; ^{1}H NMR (300 MHz, DMSO-d_6) δ 11.91 (s, 1 H), 11.78 (s, 1 H), 10.82 (s, 1 H), 7.86 (d, *J* = 16.3 Hz, 1 H), 7.57 (d, *J* = 8.1 Hz, 1 H), 7.49 (s, 1 H), 7.41 (d, *J* = 8.1 Hz, 1 H), 7.27 (d, *J* = 16.3 Hz, 1 H); ^{13}C NMR (75 MHz, DMSO-d_6) δ 167.2, 157.2, 157.1, 149.9, 148.0, 137.8, 133.5, 130.1, 126.8, 125.0, 120.4, 116.9, 116.1; negative-ion EIMS m/z 637 [(2 M − H$^+$)$^−$, 100], 318 [(M − H$^+$)$^−$, 27]. Anal. Calcd for C$_{13}$H$_9$N$_3$O$_7$·0.5H$_2$O: C, 47.57; H, 3.07; N, 12.80. Found: C, 47.35; H, 2.85; N, 12.56.

(E)-6-(2-Fluoro-3-methoxystyryl)-5-nitropyrimidine-2,4(1H,3H)-dione (38). A yellow amorphous solid **38** (115 mg, 65%): mp 318–320 °C; ^{1}H NMR (300 MHz, DMSO-d_6) δ 11.88 (s, 1 H), 11.85 (s, 1 H), 7.82 (d, J = 16.5 Hz, 1 H), 7.31 (t, J = 6.9 Hz, 1 H), 7.26 (m, 1 H), 7.21 (m, 1 H), 7.04 (d, J = 16.5 Hz, 1 H); ^{13}C NMR (75 MHz, DMSO-d_6) δ 156.4, 151.2, 149.9, 147.8, 134.0, 127.0, 125.1, 122.9, 119.2, 116.4, 115.6, 56.5; negative-ion EIMS m/z 613 [(2 M − H$^+$)$^-$, 16], 306 [(M − H$^+$)$^-$, 100]. Anal. Calcd for C$_{13}$H$_{10}$FN$_3$O$_5$: C, 50.82; H, 3.28; N, 13.68; F, 6.18. Found: C, 50.46; H, 3.15; N, 13.44; F, 5.94.

(E)-5-Nitro-6-[2-(1H-pyrrol-2-yl)vinyl]pyrimidine-2,4(1H,3H)-dione (40). A black amorphous solid **40** (0.49 g, 68%): mp 302–304 °C dec; ^{1}H NMR (300 MHz, DMSO-d_6) δ 7.71 (d, J = 16.0 Hz, 1 H), 7.13 (m, 2 H), 6.58 (d, J = 16.0 Hz, 1 H), 6.53 (m, 1 H), 6.21 (m, 1 H); ^{13}C NMR (75 MHz, DMSO-d_6) δ 156.8, 149.5, 147.9, 133.3, 132.4, 128.8, 117.52, 110.8, 105.2; negative-ion EIMS m/z 495 [(2 M − H$^+$)$^-$, 77], 247 [(M−H$^+$)$^-$, 100]. Anal. Calcd for C$_{10}$H$_8$N$_4$O$_4$: C, 48.39; H, 3.25; N, 22.57. Found: C, 48.17; H, 3.51; N, 22.85.

(E)-6-(2-(Naphthalen-2-yl)vinyl)-5-nitropyrimidine-2,4(1H,3H)-dione (43). A yellow amorphous solid **43** (0.66 g, 73%): mp 320–322 °C; ^{1}H NMR (300 MHz, DMSO-d_6) δ 11.73 (brs, 2 H), 8.11 (s, 1 H), 7.99 (m, 1 H), 7.93 (m, 1 H), 7.91 (d, J = 16.2 Hz, 1 H), 7.79 (d, J = 8.5 Hz, 1 H), 7.55 (m, 2 H), 7.13 (d, J = 16.2 Hz, 1 H); ^{13}C NMR (75 MHz, DMSO-d_6) δ 157.0, 150.2, 149.1, 141.2, 133.8, 132.9, 132.0, 129.8, 128.8, 128.6, 127.7, 127.5, 126.9, 126.3, 123.8, 115.4; negative-ion EIMS m/z 639 [(2 MNa − 2H$^+$)$^-$, 100], 617 [(2 M − H$^+$)$^-$, 22], 308 [(M−H$^+$)$^-$, 30]. Anal. Calcd for C$_{16}$H$_{11}$N$_3$O$_4$·0.75 H$_2$O: C, 59.54; H, 3.90; N, 13.02. Found: C, 59.18; H, 3.46; N, 12.83.

(E)-6-(2-(3H-Indol-3-yl)vinyl)-5-nitropyrimidine-2,4(1H,3H)-dione (44). A red amorphous solid **44** (0.62 g, 71%): mp 340–342 °C; ^{1}H NMR (300 MHz, DMSO-d_6) δ 12.10 (s, 1 H), 11.68 (s, 1 H), 11.53 (s, 1 H), 8.15 (d, J = 16.5 Hz, 1 H), 7.98 (d, J = 2.1 Hz, 1 H), 7.79 (d, J = 7.9 Hz, 1 H), 7.49 (d, J = 7.9 Hz, 1 H), 7.22 (m, 2 H), 6.85 (d, J = 16.5 Hz, 1 H); ^{13}C NMR (75 MHz, DMSO-d_6) δ 157.0, 149.6, 148.7, 137.8, 137.5, 132.5, 125.2, 124.6, 123.1, 121.6, 119.5, 112.9, 112.8, 106.3; negative-ion EIMS m/z 319 [(MNa − 2H$^+$)$^-$, 66], 297 [(M − H$^+$)$^-$, 8]. Anal. Calcd for C$_{14}$H$_{10}$N$_4$O$_4$: C, 56.38; H, 3.38; N, 18.78. Found: C, 56.10; H, 3.22; N, 18.76.

6-(Benzylamino)-5-nitropyrimidine-2,4(1H,3H)-dione (45). 6-Chloro-5-nitrouracil (**52**) (0.15 g, 0.78 mmol), benzylamine (0.09 mL, 0.86 mmol), and Et$_3$N (0.3 mL, 2.35 mmol) in 1,4-dioxane (5 mL) were heated at reflux for 12 h. The mixture was cooled to room temperature, filtered, and washed with methanol (5 mL) and ether (10 mL). The salt was dissolved in dilute KOH solution and acidified with an excess of hydrochloric acid, and the solid was filtered and washed with water (2 × 10 mL), methanol (2 × 10 mL), and then with ether (2 × 10 mL) and dried to yield a white amorphous solid **45** (145 mg, 73%): mp 284–286 °C; ^{1}H NMR (300 MHz, DMSO-d_6) δ 7.30 (m, 5 H), 4.71 (s, 2 H); ^{13}C NMR (75 MHz, DMSO-d_6) δ 157.1, 154.2, 147.6, 136.3, 128.7, 127.3, 126.4, 109.2, 46.5; EIMS m/z (rel intensity) 285 (MNa$^+$, 100), 263 (MH$^+$, 7); negative-ion EIMS m/z (rel intensity) 261 [(M − H$^+$)$^-$, 100], 227 (7). Anal. Calcd for C$_{11}$H$_{10}$N$_4$O$_4$: C, 50.38; H, 3.84; N, 21.37. Found: C, 50.04; H, 3.69; N, 21.05.

6-(2-Hydroxybenzylamino)-5-nitropyrimidine-2,4(1H,3H)-dione (46). 6-Chloro-5-nitrouracil (**52**) (0.27 g, 1.4 mmol), 2-hydroxy-benzylamine (0.19 g, 1.56 mmol), and Et$_3$N (0.6 mL, 4.23 mmol) in 1,4-dioxane (6 mL) were heated at reflux for 12 h. The mixture was cooled to room temperature, filtered, and washed with methanol (5 mL) and ether (10 mL). The salt was dissolved in dilute KOH solution and acidified with an excess of hydrochloric acid, and the solid was filtered and washed with water (2 × 10 mL), methanol (2 × 10 mL), and then with ether (2 × 10 mL) and dried to give a pale-yellow amorphous solid **46** (0.25 g, 64%): mp 138–140 °C; ^{1}H NMR (300 MHz, DMSO-d_6) δ 9.84 (t, J = 5.4 Hz, 1 H), 9.72 (brs, 1

H), 7.25 (dd, J = 1.3 Hz, 7.3 Hz, 1 H), 7.12 (m, 1 H), 6.75 (m, 2 H), 4.43 (d, J = 6.1 Hz, 2 H); ^{13}C NMR (75 MHz, DMSO-d_6) δ 159.0, 158.7, 156.1, 130.7, 128.8, 125.4, 118.8, 116.7, 66.4; EIMS m/z (rel intensity) 579 (2 MNa$^+$, 20), 380 (100), 301 (MNa$^+$, 10); negative-ion EIMS m/z (rel intensity) 555 [(2 M − H$^+$)$^-$, 100], 278 (M, 10), 277 [(M − H$^+$)$^-$, 85], 241. Anal. Calcd for C$_{11}$H$_{10}$N$_4$O$_5$: C, 47.49; H, 3.62; N, 20.14. Found: C, 47.61; H, 3.69; N, 19.83.

6-(2-Hydroxy-2-phenethyl)-5-nitropyrimidine-2,4(1H,3H)-dione (47). Lindlar catalyst (5 mg) was added to a solution of compound **9** (100 mg, 0.36 mmol) in MeOH (5 mL). A hydrogen balloon was attached, and the mixture was stirred at room temperature for 12 h. The reaction mixture was filtered through Celite, which was then washed with MeOH (2 × 5 mL). The solution was concentrated, and the residue was washed several times with CH$_2$Cl$_2$ (3 × 10 mL) and THF (3 × 10 mL). Finally, compound **47** was precipitated out by dissolving in MeOH and adding excess diethyl ether to furnish the pure product (78 mg, 78%) as a pale yellow amorphous solid: mp 231–234 °C; ^{1}H NMR (300 MHz, MeOH-d_4) δ 7.06 (m, 2 H), 6.76 (m, 2 H), 2.88 (d, J = 6.8 Hz, 1 H), 2.85 (d, J = 5.6 Hz, 1 H), 2.70 (d, J = 5.6 Hz, 1 H), 2.67 (d, J = 6.8 Hz, 1 H); ^{13}C NMR (75 MHz, MeOH-d_4) δ 163.6, 156.4, 152.0, 135.8, 131.2, 128.9, 127.7, 120.7, 119.0, 116.0, 29.8, 29.1; negative-ion ESI-MS m/z (rel intensity) 276 [(M−H$^+$)$^-$, 100], 258 (15); HRMS m/z calcd for C$_{12}$H$_{11}$N$_3$O$_5$ (M − H$^+$)$^-$ 276.0620, found 276.0619. Anal. Calcd for C$_{12}$H$_{11}$N$_3$O$_5$: C, 51.99; H, 4.00; N, 15.16. Found: C, 51.78; H, 4.28; N, 15.04.

6-(4-Hydroxy-2-phenethyl)-5-nitropyrimidine-2,4(1H,3H)-dione (48). Lindlar catalyst (5 mg) was added to a solution of compound **16** (100 mg, 0.36 mmol) in MeOH (5 mL). A hydrogen balloon was attached, and the mixture was stirred at room temperature for 12 h. The reaction mixture was filtered through Celite, which was then washed with MeOH (2 × 5 mL). The solution was concentrated, and the residue was washed several times with CH$_2$Cl$_2$ (3 × 10 mL) and THF (3 × 10 mL). Finally, compound **48** was precipitated out by dissolving in MeOH and adding excess diethyl ether to furnish the pure product (70 mg, 70%) as a yellowish amorphous solid: mp 235–237 °C; ^{1}H NMR (300 MHz, MeOH-d_4) δ 7.06 (d, J = 8.4 Hz, 2 H), 6.69 (d, J = 8.4 Hz, 2 H), 2.80 (d, J = 6.5 Hz, 1 H), 2.77 (d, J = 5.6 Hz, 1 H), 2.68 (d, J = 5.6 Hz, 1 H), 2.65 (d, J = 6.5 Hz, 1 H); ^{13}C NMR (75 MHz, MeOH-d_4) δ 163.7, 157.0, 152.0, 135.4, 132.4, 130.5, 119.0, 116.3, 33.0, 31.9; negative-ion ESI-MS m/z (rel intensity) 276 [(M− H$^+$)$^-$, 100], 258 (33); negative-ion HRMS m/z calcd for C$_{12}$H$_{11}$N$_3$O$_5$ (M − H$^+$)$^-$ 276.0620, found 276.0623. Anal. Calcd for C$_{12}$H$_{11}$N$_3$O$_5$: C, 51.99; H, 4.00; N, 15.16. Found: C, 51.91; H, 4.21; N, 14.95.

5-Nitro-6-[(3-oxo-1,3-dihydroisobenzofuran-1-yl)methyl]pyrimidine-2,4-(1H,3H)-dione (49). A pale-yellow amorphous solid **49** (0.3 mg, 68%): mp 335–337 °C. ^{1}H NMR (300 MHz, DMSO-d_6) δ 7.74 (m, 2 H), 7.56 (m, 2 H), 5.92 (dd, J = 3.0, 9.6 Hz, 1 H), 3.50 (dd, J = 3.3, 13.8 Hz, 1 H), 2.86 (dd, J = 9.6, 13.8 Hz, 1 H); ^{13}C NMR (75 MHz, DMSO-d_6) δ 169.1, 156.4, 151.7, 149.1, 148.2, 134.8, 130.0, 128.0, 125.2, 125.0 122.8, 78.2, 35.1; negative-ion EIMS m/z (rel intensity) 302 [(M−H$^+$)$^-$, 100], 170 (61). Anal. Calcd for C$_{13}$H$_9$N$_3$O$_6$: C, 51.49; H, 2.99; N, 13.86. Found: C, 51.12; H, 3.08; N, 13.57.

5-Amino-(2-hydroxy-2-phenethyl)pyrimidine-2,4-(1H,3H)-dione (50). Concentrated HCl (0.5 mL) and 10% Pd/C (30 mg) were added to a solution of 5-nitro-6-styryluracil (**39**) (300 mg, 1.16 mmol) in MeOH (10 mL). A hydrogen balloon was attached, and the mixture was stirred at room temperature for 24 h. The reaction mixture was filtered through Celite, which was then washed with 50% aq MeOH (5 mL) to provide compound **50** as a white solid (225 mg, 73%): mp 251–254 °C; ^{1}H NMR (300 MHz, MeOH-d_4/D$_2$O) δ 7.27 (m, 4 H), 7.23 (m, 1 H), 2.97 (m, 2 H), 2.85 (m, 2 H); ^{13}C NMR (75 MHz, MeOH-d_4/D$_2$O) δ 160.1, 151.4, 150.1, 140.6, 129.8, 129.5, 127.9, 115.2, 34.4, 31.8; EIMS m/z (rel intensity) 231 (M$^+$, 51), 140 (M$^+$ - C$_7$H$_7$, 80), 91 (M$^+$ − C$_5$H$_6$N$_3$O$_2$, 100); CIMS

TABLE 2. Enzymes Used in Kinetic Assays

enzyme	organism	specific activity (μmol mg^{-1} h^{-1})	concn of enzyme in reaction mixture (μg mL^{-1})
lumazine synthases:	*S. pombe*	6.8	1.0
	M. tuberculosis	0.8	30
riboflavin synthases:	*E. coli*	21	0.8
	M. tuberculosis	4.0	4.0

m/z (rel intensity) 232 (MH$^+$, 100). Anal. Calcd for C$_{12}$H$_{14}$ClN$_3$O$_2$: C, 53.84; H, 5.27; N, 15.70. Found: C, 53.99; H, 5.01; N, 15.90.

5-Amino-6-(2-hydroxyphenethyl)pyrimidine-2,4(1*H*,3*H*)-dione Hydrochloride (51). Pd/C (5 mg) was added to a solution of compound **9** (100 mg, 0.36 mmol) in MeOH (20 mL). The mixture was shaken in a Parr apparatus at 30 psi under H$_2$ atmosphere for 24 h. The reaction mixture was filtered through Celite, which was then washed with MeOH (2 × 10 mL). The solution was concentrated, and the residue was washed several times with CH$_2$Cl$_2$ (3 × 10 mL) and THF (3 × 10 mL). Finally, compound **51** was precipitated out by dissolving it in MeOH and adding excess diethyl ether to furnish pure compound **51** (65 mg, 72%) as a yellow amorphous solid: mp 239−241 °C dec; ^{1}H NMR (300 MHz, MeOH-d_4) δ 7.06 (m, 2 H), 6.75 (m, 2 H), 2.88 (d, J = 6.8 Hz, 1 H), 2.85 (d, J = 5.9 Hz, 1 H), 2.70 (d, J = 5.9 Hz, 1 H), 2.68 (d, J = 6.8 Hz, 1 H); EIMS m/z (rel intensity) 248 (MH$^+$, 100), 194 (10), 230; HRMS m/z calcd for C$_{12}$H$_{14}$N$_3$O$_3$ (MH$^+$) 248.1035, found 248.1034. Anal. Calcd for C$_{12}$H$_{14}$ClN$_3$O$_3$: C, 50.80; H, 4.97; N, 14.81. Found: C, 50.91; H, 4.81; N, 14.95.

Lumazine Synthase Assay. Assay mixtures contained 50 mM Tris hydrochloride, pH 7.0, 100 mM NaCl, 2% (v/v) DMSO, 5 mM dithiothreitol, 100 μM **2**, lumazine synthase (Table 2), variable concentrations of **1** (3−150 μM), and inhibitor (0−150 μM) in a volume of 0.2 mL. Assay mixtures were prepared as follows. A solution (175 μL) containing 103 mM NaCl, 5.1 mM dithiothreitol, 114 μM **2**, and lumazine synthase in 51 mM Tris hydrochloride, pH 7.0, was added to 4 μL of inhibitor in 100% (v/v) DMSO in a well of a 96-well microtiter plate. The reaction was started by adding 21 μL of a solution containing 103 mM NaCl, 5.1 mM dithiothreitol, and substrate **1** (30−1500 μM) in 51 mM Tris hydrochloride, pH 7.0. The formation of 6,7-dimethyl-8-D-ribityllumazine (**3**) was measured online for a period of 40 min at 27 °C with a computer-controlled plate reader at 408 nm ($\varepsilon_{\text{lumazine}}$ = 10200 M^{-1} cm^{-1}).

Riboflavin Synthase Assay. Assay mixtures contained 50 mM Tris hydrochloride, pH 7.0, 100 mM NaCl, 2% (v/v) DMSO, 5 mM dithiothreitol, enzyme (Table 2), variable concentrations of **3** (3−20 μM), and inhibitor (0−150 μM) in a volume of 0.2 mL.

Assay mixtures were prepared as follows. A solution (175 μL) containing 103 mM NaCl, 5.1 mM dithiothreitol, and riboflavin synthase in 51 mM Tris hydrochloride, pH 7.0, was added to 4 μL of inhibitor in 100% (v/v) DMSO in a well of a 96-well microtiter plate. The reaction was started by adding 21 μL of a solution containing 103 mM NaCl, 5.1 mM dithiothreitol, and substrate **3** (30 − 200 μM) in 51 mM Tris hydrochloride, pH 7.0. The formation of riboflavin was measured online for a period of 40 min at 27 °C with a computer-controlled plate reader at 470 nm ($\varepsilon_{\text{riboflavin}}$ = 9600 M^{-1} cm^{-1}).

Details of the Assay Procedures. For both lumazine synthase and riboflavin synthase assays, four different inhibitor concentrations and seven different substrate concentrations were used. Therefore, a series of measurements for one compound included 28 sample reactions plus four reactions without substrate added (as control samples). The enzyme was added before the reaction mixture was pipetted into different wells on a 96-well microtiter plate. The enzyme concentration in all reaction mixtures was identical. After enzyme was added, the solution was divided into four parts, and a different amount of inhibitor was added to each of them. The accuracy of the measurements on the plate reader was checked regularly. An identical amount of substrate was added to every well on the microtiter plate containing identical enzyme solutions. The results of measurements were analyzed for all wells, and standard deviation values were between 3% and 8%. The standard deviation values in Table 1 are important criteria for determining the mode of inhibition and do not reflect the accuracy of pipetting or photometric measurements.

Evaluation of Kinetic Data. The velocity-substrate data were fitted for all inhibitor concentrations with a nonlinear regression method using the program DynaFit.[34] Different inhibition models were considered for the calculation. K_i and K_{is} values ± standard deviations were obtained from the fit under consideration of the most likely inhibition model as described previously.[17]

Supporting Information Available: ^{1}H NMR and ^{13}C NMR spectra of **9**, **14−23**, and **25−51**. This material is available free of charge via the Internet at http://pubs.acs.org.

(34) Kuzmic, P. *Anal. Biochem.* **1996**, *237*, 260−273.